arXiv:0807.3542v1 [astro-ph] 22 Jul 2008

Outburst Morphology in the Soft X-ray Transient Aquila X-1

Dipankar Maitra

Sterrenkundig Instituut "Anton Pannekoek", University of Amsterdam, Kruislaan 403, 1098 SJ Amsterdam, The Netherlands

`D.Maitra@uva.nl`

and

Charles D. Bailyn

Yale University, Department of Astronomy, P.O.Box 208101, New Haven, CT 06520-8101, USA

`charles.bailyn@yale.edu`

ABSTRACT

We present optical and near-IR (OIR) observations of the major outbursts of the neutron star soft X-ray transient binary system Aquila X-1, from summer 1998 – fall 2007. The major outbursts of the source over the observed timespan seem to exhibit two main types of light curve morphologies, (a) the classical *Fast-Rise and Exponential-Decay* (FRED) type outburst seen in many soft X-ray transients and (b) the *Low-Intensity State* (LIS) where the optical-to-soft-X-ray flux ratio is much higher than that seen during a FRED. Thus there is no single correlation between the optical (R-band) and soft X-ray (1.5-12 keV, as seen by the ASM onboard RXTE) fluxes even within the hard state for Aquila X-1, suggesting that LISs and FREDs have fundamentally different accretion flow properties. Time evolution of the OIR fluxes during the major LIS and FRED outbursts is compatible with thermal heating of the irradiated outer accretion disk. No signature of X-ray spectral state changes or any compact jet are seen in the OIR, showing that the OIR color-magnitude diagram (CMD) can be used as a diagnostic tool to separate thermal and non-thermal radiation from X-ray binaries where orbital and physical parameters of the system are reasonably well known. We suggest that the LIS may be caused by truncation of the inner disk in a relatively high $\dot{M}$ state, possibly due to matter being diverted into a weak outflow.

Subject headings: accretion, accretion disks — stars: neutron — stars: — X-rays: binaries — individual (Aquila X-1)

1. Introduction

Aquila X-1 is one of the most frequently recurring soft X-ray transients in the sky. It goes into outburst approximately once every year although the periodicity is not fixed (Šimon 2002). The frequent outburst recurrence makes it an ideal source for studying accretion flow during an outburst as well as changes in accretion flow from outburst to outburst. The physical and orbital parameters of this system are relatively well known. The orbital period of the binary system was determined to be 18.71 ± 0.06 hours by Welsh et al. (2000) from optical photometry during quiescence. Chevalier et al. (1999) estimated the quiescent V-band magnitude to be 21.6 ± 0.10 magnitude. However, there is a contaminating star about $0.48''$ East of Aquila X-1 which has a V magnitude of 19.42 ± 0.06 (Chevalier et al. 1999). The distance to the system is between 4-6.5 kpc as inferred both from (a) limits on optical brightness of the Roche lobe filling donor star of spectral type between K6-M0 (Chevalier et al. 1999; Rutledge et al. 2001) and (b) peak X-ray fluxes during type-1 bursts (Czerny, Czerny, & Grindlay 1987; Rutledge et al. 2001).

In systems like Aquila X-1 and other Roche lobe overflowing soft X-ray transient (SXT) binary systems, the thermal viscous disk instability model (DIM; Lasota 2001) is usually invoked to explain the typical *fast-rise and exponential-decay* (FRED) type outburst light curve morphology (Chen et al. 1997). The DIM alone however cannot produce realistic FRED outbursts. Another mechanism that plays a key role during outbursts of SXTs is X-ray irradiation. The irradiation is caused by the intense X-rays from the inner regions of the accretion disk and neutron star surface (if the system harbors a neutron star) impinging on the outer disk/donor, and by re-emission of this impinged energy in lower energies (Cunningham 1976; Vrtilek et al. 1990; van Paradijs & McClintock 1994; McClintock et al. 1995; Dubus et al. 1999; O'Brien et al. 2002; Hynes et al. 2002; Russell et al. 2006). Another catagory of modifications to the DIM is generated by the possible truncation of the inner region of the accretion flow, where the disk inflow can be replaced by a radiatively inefficient accretion flow (RIAF). There is an increasing body of work on this topic (Ichimaru 1977; Rees et al. 1982; Narayan & Yi 1994; Blandford & Begelman 1999; Meier 2001), but the overall impact of these efforts on the outburst morphology is currently still unclear.

Collimated relativistic outflows, loosely termed as "jets", have been observed in several soft X-ray transients (see Fender 2006, for a review) and their broad band spectral energy distribution (SED) from radio to X-rays have been fitted with jet+disk models comprising of a freely expanding "Blandford - Königl" jet (Blandford & Königl 1979; Falcke & Biermann 1999; Markoff et al. 2005) and a thermal-viscous "Shakura-Sunyaev" accretion disk (Shakura & Sunyaev 1973). Observations suggest that compared to black hole (BH) systems, the neutron star (NS) SXTs tend to have intrinsically weaker jets and also the transition from optically-thick to optically-thin jet spectrum in NS systems probably occurs in the mid-IR (Migliari & Fender 2006; Migliari et al. 2006, this work), compared to that in near-IR for BH systems (Corbel & Fender 2002; Buxton & Bailyn 2004; Homan et al. 2005; Russell et al. 2006).

During outburst, light curve morphology of many sources are not FREDs. The X-ray spectral and temporal features also show an enormous diversity during outbursts of SXT systems, and are categorized into various *states*. See e.g. McClintock & Remillard (2006) and Homan & Belloni (2005) for extensive discussions on definition of states and van der Klis (2006) for their timing properties. Despite the multitude of states observed in the different systems and different outbursts, two "canonical" states can be identified during the outburst of most SXTs, characterised by presence or absence of a thermal and nonthermal component in the energy spectrum. In the temporal domain, presence or absence of a thermal component usually shows up respectively as low or high rms variability in the light curve. A host of other intermediate and extreme states are also seen, which could be a superposition of the thermal and nonthermal components with varying contributions. Precise determination of X-ray state requires modeling of spectral energy distribution and Fourier power density spectra. Since this work primarily focusses mainly on OIR observations, we have used dates of X-ray state transitions of Aquila X-1 from published studies of X-ray spectral and temporal properties of the source (Maccarone & Coppi 2003a,b; Reig et al. 2004; Maitra & Bailyn 2004; Rodriguez et al. 2006; Yu & Dolence 2007) to study correlation between X-ray state and OIR flux-density.

We have observed Aquila X-1 for $\sim$ 9 years, through many outbursts, to explore the nature of outburst morphologies in a single object. Even though the OIR (as well as X-ray) light curve morphologies from outburst to outburst differ, we find systematic and repeated tracks traced by the source in OIR color-magnitude diagrams. Since we have long-term data in two bandpasses (R and J) only, we have used a simple model to show that the color evolution and the resulting track are consistent with heating of a constant area blackbody and can be caused by an irradiated outer disc.

In §2 we describe the general reduction procedures adopted in this work. The light curve morphologies in J, R and ASM bands (of the RXTE satellite) and optical–soft X-ray correlations during the major outbursts are described in §3. Evolution of Aquila X-1 on the OIR color-magnitude diagram is presented in §4. Finally we present our discussions in §5.

2. Observations and Data Analysis

2.1. Optical and Near-IR data

Our long term monitoring campaign used the Yale 1.0m telescope at Cerro Tololo Inter-American Observatory (CTIO) in Chile to observe Aquila X-1 from 1998-2002 on a daily basis (weather and Sun-angle constraints permitting). Since February 2003, the CTIO 1.3m telescope has been used for the monitoring. In both cases, images were obtained using the ANDICAM[1] instrument, which is a dual-channel imager capable of simultaneously recording images at an optical and an infrared wavelength. Prior to MJD 52430 (2002 June 5), the optical R-band data were recorded by a Lick/Loral-3 2048×2048 CCD. Thereafter, the R-band has been recorded by a Fairchild 447 2048×2048 CCD. The near-IR J-band data are recorded by a Rockwell 1024×1024 HgCdTe Astronomical Wide Area Infrared Imager (HAWAII) imager. Between MJD 51130–51367 (1998 November 13 – 1999 July 8th), the source was observed using a "wide-R" filter. The wide-R filter has a broader bandpass than the Johnson R filter used during the rest of the campaign. Even though a determination of the Johnson R-band flux cannot be made from the wide-R-band measurements, the light curve morphology changes little due to the change of filter. We calculated the quiescent wide-R-band differential magnitude (between MJD 51232 and MJD 51306) and applied an offset to the differential magnitudes obtained using wide-R filter so that the quiescent level was set to 18.8 magnitude, which is the quiescent R-band magnitude of Aquila X-1.

Under normal viewing conditions at CTIO, it is extremely difficult to separate the true optical counterpart of Aquila X-1 from the bright contaminating star. Therefore the magnitudes reported in this work are the combined magnitudes of the Aquila X-1 system and the contaminating star, and when we say magnitude of Aquila X-1 we actually mean the combined magnitude of Aquila X-1 and the contaminating star. In quiescence, light from the contaminating star dominates, but once an outburst begins, photons from Aquila X-1 dominate.

The optical data reduction, including bias subtraction, overscan correction, and flat-fielding, was done through the standard IRAF data reduction pipeline developed for these instruments[2]. For the J-band near-IR data, multiple dithered frames were taken and then flat-fielded, sky subtracted, aligned and average-combined using an in-house IRAF script. During a large portion of the year 2004, one of the four quadrants of the IR CCD was not working. In most of the observations during this period, one or more of the reference stars were not present in the frames. We used whichever comparison stars were present and adjusted the resulting differential magnitudes appropriately.

---

[1] http://www.astro.yale.edu/smarts/ANDICAM

[2] For details see http://www.astro.yale.edu/smarts/smarts13m/optprocessing.txt

We used the field stars 2MASS 19111739+0035039 and 2MASS 19111633+0034333 with J-band magnitudes of 12.404 and 12.490 respectively[3], to obtain differential magnitude of the source. Flux calibration of these reference stars in the R-band was performed by comparing with Landolt standard stars on the photometric night of MJD 53904 (2006 June 18). In order to estimate time variability in flux from any of the reference stars, we calculated the difference between the observed magnitudes of the reference stars on every night. Smaller than 0.02 mag in R-band, this difference is the primary source of error in flux determination because during outbursts the Poisson error due to photon count-rate is much smaller. The S/N is even better in J-band where interstellar extinction is lesser.

For magnitude to flux conversion, following Bessell et al. (1998) and Campins et al. (1985), we assumed that R=0 magnitude converts to 3064 Jy and J=0 magnitude converts to 1603 Jy. Welsh et al. (2000) estimated that $83 \pm 2\%$ of the quiescent R-band flux is from the contaminating star. Assuming that the brightness of the contaminating star is constant in time, we subtracted this flux from the total observed flux to obtain the flux of Aquila X-1 only, during quiescence as well as outbursts. Interstellar reddening and extinction was calculated assuming a hydrogen column density (N_H) of 3.4×10^{21} atoms/cm^2 in the direction of Aquila X-1 (Dickey & Lockman 1990). From deep optical photometry and spectroscopy of the source during quiescence Chevalier et al. (1999) estimated the color excess $E(B-V) = 0.5 \pm 0.1$ which is consistent with the Dickey & Lockman (1990) value of N_H in the direction of Aquila X-1. For dereddening the OIR flux we used the standard N_H to visual extinction (A_V) correlation given by $N_H/A_V = 1.79 \times 10^{21}$ atoms/cm^2/mag (Predehl & Schmitt 1995) and the extinction law of Cardelli et al. (1989) which gives $A_R/A_V = 0.748$ magnitude and $A_J/A_V = 0.282$ magnitude for Aquila X-1. Taking reddening and extinction in the direction of Aquila X-1 into account, the observed $R-J$ color is linearly related to the corresponding intrinsic spectral index ($\alpha_{RJ;int}$) by the relation

$$\alpha_{RJ;int} = \frac{log(f_R) - log(f_J)}{log(\nu_R) - log(\nu_J)} = 2.47 - 1.63 \times (R-J)_{observed}. \qquad (1)$$

2.2. X-ray data

The X-ray data was taken from the All Sky Monitor (ASM; Levine et al. 1996) aboard the Rossi X-ray Timing Explorer (RXTE; Jahoda et al. 1996) satellite. The ASM has been monitoring the sky in the 1.5-3, 3-5 and 5-12 keV energy bands continuously since 1996. Usually a given source is observed a few times every day, subject to constraints like angular proximity to the Sun etc. The results are made publicly available by the MIT/ASM team through their website[4]. We have used the one day average light curve for Aquila X-1. During quiescence, the flux from Aquila X-1 is below the detection limit of the ASM, however since we are interested only in the major outbursts, which are detectable by the ASM, we did not take into account data during quiescence, for our optical-X-ray correlation study. Also, during the early as well as the late stages of the outbursts, the count-rates in the individual energy channels are small; therefore we have only looked at the summed count-rates in this work. The ASM count-rates were converted to flux-density at 5.2 keV, assuming a Crab-like spectrum. The Crab spectrum in the ASM energy range is a simple power law with a photon-index of -2.1 and the total flux within that range is 2.8×10^{-8} ergs/cm^2/s (Smith et al. 2002), so the flux-density at 5.2 keV is 1.06 mJy. The flux conversion (from ASM count-rate to μJy) is therefore a numerical factor by which the total ASM count rate is multiplied. The choice of 5.2 keV was motivated by the fact that it is the geometric mean of the half-transmission points of the ASM response shape[5] near 2.3 and 12 keV. We used geometric mean (GM) because the GM compensates for the fact that almost all X-ray spectra slope downward in count rate toward higher energies.

---

[3] Taken from the 2MASS point source catalogue at http://www.ipac.caltech.edu/2mass

Evolution of spectral shape during an outburst introduces uncertainities in flux determination. Pivoting uncertainities (due to spectral evolution) in ASM's X-ray range are small compared to the optical to X-ray separation in frequency space. We used the online *WebPIMMS*[6] tool which shows that for a given total ASM count-rate, the difference in flux in the ASM band-pass is less than 10% between a power law of photon index 2.1 (i.e. Crab spectrum), a power law of photon index 1.7 or a blackbody at 2 keV (typical photon index/blackbody temperature of Aquila X-1 in hard/soft state; see e.g. Maccarone & Coppi 2003b; Maitra & Bailyn 2004; Rodriguez et al. 2006). Therefore we added a 10% systematic error, in quadrature to the Poisson error, during the ASM count-rate to flux conversion to account for the uncertainity in the spectral shape. The precise value for pinning and rescaling the flux conversion is not very sensitive to the choice of keV reference, as long as this is done self-consistently (i.e. scale to Crab flux density at the reference keV, and implemented in this work).

---

[4] http://xte.mit.edu

[5] Taken from appendix F of the RXTE technical appendix (http://heasarc.nasa.gov/docs/xte/appendix_f.html) and Ron Remillard, priv. comm.

[6] http://heasarc.gsfc.nasa.gov/Tools/w3pimms.html

In this process, any information about changes in the energy spectrum is lost, but we are primarily concerned with overall X-ray flux here, and using all the counts results in better signal-to-noise ratio. In order to assess the X-ray state of the source, we have used the dates of state transitions from published literature Maccarone & Coppi (2003a,b); Reig et al. (2004); Maitra & Bailyn (2004); Rodriguez et al. (2006); Yu & Dolence (2007). For the most recent outbursts (e.g. outburst #9, #10) with no published dates of state transition(s), we used the (9.7-16 keV/6-9.7 keV) hardness ratio from archival RXTE/PCA pointed observations (Manuel Linares, priv. comm.) whose value correlates strongly with the X-ray state of the source. For outbursts with sparse coverage of pointed observations (e.g. outburst #5) we used the (5-12 keV/3-5 keV) hardness ratio from the RXTE/ASM data to infer the spectral state.

3. Major Outbursts of Aquila X-1 since 1998 June 20

In Fig. 1 we show the results of long-term multi-wavelength monitoring of Aquila X-1. The RXTE/ASM monitoring of Aquila X-1 dates back to the beginning of 1996, but our nightly R-band monitoring started on MJD 50984 (1998 June 20th). The J-band observations started MJD 51677 (2000 May 13th) onwards, but the coverage was somewhat sporadic till the end of 2002, as can be seen from the top panel of Fig. 1. During quiescent periods, the system is detected in both of the OIR bands but not in ASM. Therefore in Fig. 1 we have only plotted those ASM points for which the signal-to-noise ratio is better than four.

Since observing constraints sometimes make it difficult to date the precise starting and ending moments of an outburst, in Table 1 we note the MJD when the ASM, R-band and J-band fluxes attained a maximum during an outburst. We define a major outburst as a period of activity of the source, spanning at least 20 days or longer, when the source flux was at least 3σ above quiescence in at least one of the observed (J, R and ASM) bandpasses. Eleven major periods of activity were observed by the ASM during this period. All these periods of major activity were also seen in OIR, except the one during late 2005–early 2006 when the source's angular proximity to the Sun was too close to observe with ground based OIR telescopes. Even the RXTE/ASM data, while showing unmistakeable signs of activity during this particular outburst, does not have sufficient coverage and S/N to classify the light curve morphology.

Besides the major outbursts, several smaller and shorter periods of activity are seen in the OIR light curve (Fig. 1). Because of the low signal-to-noise ratio, particularly in ASM data, and scarcity of PCA pointings during these periods of minor activity, they have not been discussed in the present work. However, the time of peak OIR flux from the source during these “mini” outbursts have been presented in Table 1.

3.1. Lightcurve morphology: FREDs and LISs

From the long-term OIR monitoring of Aquila X-1 from MJD 50984 – MJD 54411 (1998 June 20 – 2007 Nov 7) only three out of the major OIR outbursts are purely FREDs. The remaining are a combination of FREDs with another active state where the flux is above quiescence, but does not rise or decay on the timescale of a FRED. Instead, a plateau type light curve with significant variability on a timescale of days is seen in all bands. Sometimes this state persists significantly longer than the FREDs. For Aquila X-1 the typical observed FRED rise times are ∼ few days to a week and the decay times are ∼ 3–4 weeks. On the other hand, the longer lasting, somewhat variable state can last for longer than a month. Following Wachter et al. (2002), who reported observation of such state in the neutron star system X1608-52, we call this a “Low-Intensity State” (LIS). In Fig. 2 – Fig. 5 we show blowups of the R-band and ASM light curves for each of the major outbursts in Fig. 1 (also tabulated in Table 1). FREDs and LISs are shown by different symbols in Fig. 2 – Fig. 5. During a LIS, the OIR flux is near the maximum, but always slightly lower than the corresponding maximum flux observed during a pure FRED outburst. For LISs, the variability in the light curve is more complicated than the typical ‘up to a maximum, then down to quiescence’ morphology seen for FREDs. For a comparable optical brightness, the soft X-ray flux is a factor of seven or more lower in a LIS than in a FRED. This high optical-to-X-ray flux-ratio, discussed in greater detail in §3.2, is one of the defining characteristics of a LIS.

3.2. Optical–soft X-ray correlations

The strongest evidence for the existence of an independent LIS comes from optical–X-ray correlations. From the long-term OIR monitoring data, we estimated R-band flux-density from Aquila X-1 as described in §2.1. The RXTE/ASM one day averaged count-rates were converted to flux-density as well (§2.2). Both light curves were then searched for quasi-simultaneous optical–X-ray data where the observation times in each bandpass were not separated by more than one day. In Fig. 6 we show the optical–soft-X-ray flux correlation during the major outbursts for which we had quasi-simultaneous ASM and R-band data.

The optical and soft-X-rays increase approximately linearly with $f_{opt}/f_{X-ray} \sim 1.3-1.5$ for FRED outbursts and $\sim 9-12$ for the LISs. Given the considerable scatter in the data, we have not attempted to fit the data with any function and the flux-ratios quoted above, as shown in Fig. 6, are a guide to the eye. For the same X-ray brightness, there is no strong hint of hysteresis, i.e. the optical brightness during outburst rise is not significantly different from than that during the outburst decline. The absence of optical–X-ray hysteresis in Aquila X-1, goes to support the hypothesis that either jets in neutron star systems are generally weaker or the jet break occurs at a lower frequency (Migliari & Fender 2006; Migliari et al. 2006; Russell et al. 2007).

Both FREDs and LISs start/end the outburst at quiescence and hence have a common start/end-point near the lower-left region of $f_{opt} - f_{X-ray}$ plane. For some of the weakest outbursts, the ASM fluxes are within a few sigma of detection threshold. At such low luminosities, both FREDs and LISs occupy similar regions on the $f_{opt} - f_{X-ray}$ plane. It has been observed that for some low luminosity outbursts, the source may never come out of the X-ray hard state during the entire period of activity (e.g. see Rodriguez et al. 2006). Even though the peak optical brightnesses of the brightest LISs are comparable to the peak optical brightness during FREDs, LISs are typically fainter than FREDs. The distinction between LIS and FRED outbursts stands out clearly when optical and X-ray data from *all* the major outbursts since 1999 June 20 are plotted on $f_{opt} - f_{X-ray}$ plane (Fig. 6). LISs and FREDs occupy separate regions of the $f_{opt} - f_{X-ray}$ plane and evolve on different timescales, suggesting different physical mechanisms for their origin.

4. OIR color evolution

In Fig. 7 and Fig. 8 the time evolution of the R and J-band magnitudes and that of the R−J color is shown for the major outbursts that were observed in both bandpasses. There seems to be no significant inter-band time lag during rise or decay of an outburst. Irrespective of the light curve morphology during the outburst, the R−J color is always bluer during an outburst compared to the quiescent value, and therefore $(R - J)_{outburst} < (R - J)_{quiescence}$ as seen in Fig. 7 and Fig. 8. This decrease in R−J color (becoming bluer) is characteristic of increased irradiation heating of the outer disk.

During quiescence, the disk flux is very low compared to the combined flux from the contaminating star and the donor star. It is however interesting to note that the R−J color during an LIS is significantly redder than that during the peak of a FRED outburst.

Fig. 9 and Fig. 10 shows the OIR color-magnitude diagram for the different outbursts. The R-band magnitude is plotted along the ordinate. As is typical for conventional color-magnitude diagrams, the ordinate axis has been reversed so that higher luminosities (i.e.

lower magnitude) are plotted near the top and vice-versa. The R−J color is plotted along the abscissa.

During periods of quiescence, the source flux is low and essentially dominated by photons from the contaminating star and the donor, and it lingers near the bottom-right corner of the color-magnitude diagram. As the source enters an outburst, the brightness increases and the color becomes bluer, due to an increasing contribution of the accretion disk flux. In Fig. 9 and Fig. 10, the observations when the source was in the hard state during the rise of an outburst, when it was in the hard state during the decay and when it was in the soft state are shown by different symbols. As noted in § 3.2, there are also outbursts when the source spent the entire period of activity in an X-ray hard state (Rodriguez et al. 2006). The OIR data during such outbursts are shown by open squares. There seems to be no significant change in OIR color across the X-ray spectral state transitions.

We attempted to test the simple ansatz that the observed evolution on the color-magnitude diagram is consistent with the thermal heating of a blackbody. Our goal is to see whether the flux and color variations are correlated as would be expected if the only change is in the disk temperature. For simplicity, and because we had only two band-passes, we considered the entire annulus to be a single temperature blackbody, even though real accretion disks are likely to have a significant temperature gradient. In this simple model, the R−J color is determined by the temperature of the annulus and the R-band brightness is proportional to the projected area of the annulus and inversely proportional to the square of the distance to the source. Since the observed brightness depends on the projected area, we multiplied the area of a disk of radius R_{disk}, by a multiplicative factor $f < 1$, and used this area as the area of the annulus. Thus in this simple model the brightness is proportional to $f(R_{disk}/D_{disk})^2 cos(i)$, where D_{disk} and i are the source distance and i is the orbital inclination respectively. The only adjustable parameter here is f, which changes the overall projected area of the annulus. The parameter f is changed from outburst to outburst, keeping other parameters constant. Fitting the ellipsoidal variations observed in the quiescent light curve, Robinson et al. (2001) estimated that $36° \leq i \leq 55°$. We assumed an inclination of 45°. An upper limit on R_{disk} can be presumed to be equal to the radius of the Roche lobe of the accretor and therefore can be estimated from the mass ratio and orbital period (Eggleton 1983). Evolution of the source on the color-magnitude diagram was generated by calculating the color and brightness of the annulus at varying temperature. We note that the track generated by the heating/cooling of this constant area blackbody broadly describes the evolution of the source during its outbursts. For a purely viscous disk (no irradiation) the spectral index between R and J bands (as defined in Eq. 1) should lie between 1/3 and 2. The observed range in $R - J$ color during outbursts is approximately between 1.35 and 2.1, which using Eq. 1 translates to a spectral slope between 0.27 and −0.95 respectively.

The observed range in spectral indices is quite different from what could be expected from a purely viscous disk and favors irradiation heating.

We found that even for the largest possible disk radius of ∼5 light seconds ($M_{donor} = 0.5 M_{\odot}$, $M_{accretor} = 1.5 M_{\odot}$, $P_{orb} = 18.95$ hour), the model-predicted R-band flux is too small for the lowest distance estimate of 4 kpc by Rutledge et al. (2001). Using $D_{disk} = 3$ kpc seems to lie close to the observed datapoints (see Fig. 9 and Fig. 10). Since we are not doing detailed spectral fits, we do not claim the distance to the source to be 3 kpc, but show that this very simple model can roughly predict the outburst behavior of the accretion disk. The model curves overplotted in Fig. 9 and Fig. 10 are not fits to the datapoints but created using a disk of radius 5 light-seconds, inclined at an angle of 45° to the observer and at a distance of 3 kpc from the observer, viz. a set of parameters that is generally consistent with the observed values, and with a small range (0.6-0.8) in the value of the multiplicative factor f. The general consistency of the data over many outbursts supports the idea that the OIR flux is largely due to thermal emission from an irradiated disk. This is in contrast to recent observations of accreting black hole systems in which a strongly non-thermal component is often observed in the near IR (Buxton & Bailyn 2004; Homan et al. 2005; Russell et al. 2006, Russell, Maitra & Fender, in prep.).

5. Discussion

Multi-wavelength monitoring of the neutron star soft X-ray transient Aquila X-1 in near-IR, optical and soft X-ray data from RXTE/ASM over the past nine years has allowed us to study the evolution of the source with unprecedented coverage. The OIR and X-ray light curves show a wide range of outburst light curve patterns. However the major outbursts show two distinct light curve morphologies. The *fast-rise and exponential-decay* (FRED; Chen et al. 1997) type outbursts characteristic of many soft X-ray transients is seen in Aquila X-1 too. However, only three of the major outbursts seen since 1998 June show just a FRED type light curve profile. More often a prolonged, somewhat variable "Low-Intensity state" (LIS; Wachter et al. 2002), uniquely characterized by an extremely high optical-to-soft X-ray flux-ratio, is seen either before or after a FRED. It has been observed that for some of these "soft X-ray faint" LIS outbursts, Aquila X-1 never comes out of the X-ray hard state during the entire outburst (Rodriguez et al. 2006). Other than these major outbursts, small-scale flaring activities were also observed. While the origin of such small-scale short activity remains unknown, such activity has been observed in other sources like XTE J1550-564 by Sturner & Shrader (2005) who suggested that these small outbursts could be due to discrete accretion events. We suggest the following framework for understanding these results:

Irradiation dominates OIR flux for both FRED and LIS outbursts of Aquila X-1. During the course of FRED and LIS outbursts of Aquila X-1 the evolution of the source on the OIR color-magnitude diagram is consistent with heating/cooling of an irradiated outer accretion disk as a constant area blackbody. A classical viscous accretion disk (e.g. a Shakura-Sunyaev disk) spectrum has a frequency dependence of $F_\nu \sim \nu^{1/3}$ between $kT(R_{out})/h \ll \nu \ll kT(R_{in})/h$ where $T(R_{in})$ and $T(R_{out})$ are the disc temperatures at the inner and outer edges of the disk. At frequencies much smaller than $kT(R_{out})/h$ the disk spectrum is simply the Rayleigh-Jeans region of a blackbody with $F_\nu \sim \nu^2$. For soft X-ray transients $kT(R_{in})/h$ is typically in far-UV or soft X-rays. Therefore in our case the flux ratios (a.k.a. colors) of two bands, from a purely viscous disc are expected to be constant as long as *both bands* are either on the viscous ($\nu^{1/3}$) or Rayleigh-Jeans (ν^2) regime. In the special case when the break frequency between the viscous dissipation and the Rayleigh-Jeans regime given by $\nu_{break} = kT(R_{out})/h$ lies between R and J bands, the spectral index should lie between 1/3 and 2. The observed systematic and continuous change in color (and the corresponding range in the spectral index from -0.95 to 0.27; §4) seen in Fig. 7 and Fig. 8 is strongly suggestive of an irradiative origin for the observed OIR emission and not of a purely viscous origin.

Neither the OIR color nor its brightness change sharply during an X-ray spectral state transition. This confirms that for Aquila X-1 the outer accretion disk, which emits most of the thermal OIR radiation, is not affected by X-ray spectral state transitions which change the physical environment of the inner regions of the accretion disk. This is in sharp contrast with black hole binaries like 4U 1543-47, GX 339-4 (Buxton & Bailyn 2004; Homan et al. 2005) where near IR colors are strongly correlated with X-ray state changes and the correlation interpreted as evidence for non-thermal emission. In FREDs, a slow increase in brightness above that predicted by our constant area blackbody model, as the source becomes bluer and brighter, is most likely due to increase in the surface area of the disk (e.g most prominent for outburst #2 and #5 in Fig. 9). It is possible that at highest mass accretion rates the high X-ray flux from the central inner disk causes the flaring of the outer disk and hence increase the effective surface area. In contrast, during the LISs, when the source probably spends the whole period of activity in hard X-ray state, there does not seem to be any significant change in the disk area (e.g. outburst #7 in Fig. 10). Therefore it is likely that the effect of X-ray state transition on the outer accretion disk is both an increase of the outer disk temperature due to enhanced irradiation from the inner disk and an increase in the emitting area of the outer disk due to flaring. Total irradiation (hence OIR flux) is a bit smaller in LIS than in peak FRED. This could be due either to lower $\dot{M}$, or to radiative inefficiency lowering $L/\dot{M}$ ratio.

Broad band quasi-simultaneous observations in LIS suggest outflow. Soft X-ray flux is very low in LIS, but hard X-rays are high (Molkov et al. 2004, Linares et al. in preparation,). While absence of soft, thermal X-ray photons suggests that the inner edge of the accretion disk is cold and probably receded during the LIS, the high OIR brightness (see Fig. 6 for the dramatic difference in f_{opt}/f_{X-ray} between LIS and FRED outbursts) as well as type I X-ray bursts suggests that a significant amount of mass is being accreted by the outer accretion disk and fed to the inner region.

Radio detection of the source during LIS (Rupen et al. 2004) with flat spectral slope hints toward a jet outflow. However, since the evolution of the source on OIR color-magnitude diagram is consistent with irradiation, it can be concluded that the jet, if present, is either quite weak in terms of the input power, or the transition from optically thick to optically thin jet emission occurs at a wavelength much longer than J-band. Current models for jets from compact systems suggest that this might imply a large jet launching area or the jet base, or much weaker particle acceleration (Markoff et al. 2001). Thus our observations support the current hypothesis that jet-luminosity is not significant in most neutron star X-ray binary systems (Migliari & Fender 2006; Fender 2006).

A possible scenario for the LIS might be that an $\dot{M}$ that would ordinarily be high enough to move the disk inwards, and thus trigger a soft state, somehow doesn't do that, and launches an outflow instead. Thus the standard processes associated with the DIM are disrupted by the absence of an inner disk in this high $\dot{M}$ state. If the accretion flow in the inner region in a LIS is radiatively inefficient, it can drive the observed outflow, as suggested by recent theoretical works (see e.g. Blandford & Begelman 1999; Meier 2001; Narayan 2005).

It is a pleasure to thank the SMARTS observers J. Espinoza and D. Gonzalez for taking the data over the years, and R. Winnick, J.Nelan and M. Buxton who accommodated our many requests to revise the observing schedule. We would like to thank Ron Remillard of the ASM team for his help in converting ASM count-rates to flux-density. DM would like to thank Manu Linares for providing PCA colors of all the RXTE observations of Aquila X-1 ahead of publication, and Sera Markoff, Dave Russell and Rob Fender for discussion and useful comments. We would like to thank the anonymous referee for constructive criticisms which improved the paper. DM is supported by Netherlands Organisation for Scientific Research (NWO) grant number 614000530. CDB acknowledges support from the National Science Fopundation grant nsf-ast 0707627. This work has made use of the Astrophysics Data System Abstract, the MIT/ASM data extraction website. This work has also used data products from the Two Micron All Sky Survey, which is a joint project of the University of Massachusetts and the Infrared Processing and Analysis Center/California Institute of Technology, funded by the National Aeronautics and Space Administration and the National Science Foundation.

Facilities: RXTE, SMARTS

REFERENCES

Bessell, M. S., Castelli, F., & Plez, B. 1998, A&A, 333, 231

Blandford, R. D., & Begelman, M. C. 1999, MNRAS, 303, L1

Blandford, R. D., & Königl, A. 1979, ApJ, 232, 34

Buxton, M. M., & Bailyn, C. D. 2004, ApJ, 615, 880

Campins, H., Rieke, G. H., & Lebofsky, M. J. 1985, AJ, 90, 896

Cardelli, J. A., Clayton, G. C., & Mathis, J. S. 1989, ApJ, 345, 245

Chen, W., Shrader, C. R., & Livio, M. 1997, ApJ, 491, 312

Chevalier, C., Ilovaisky, S. A., Leisy, P., & Patat, F. 1999, A&A, 347, L51

Corbel, S., & Fender, R. P. 2002, ApJ, 573, L35

Cunningham, C. 1976, ApJ, 208, 534

Czerny, M., Czerny, B., & Grindlay, J. E. 1987, ApJ, 312, 122

Dickey, J. M., & Lockman, F. J. 1990, ARA&A, 28, 215

Dubus, G., Lasota, J.-P., Hameury, J.-M., & Charles, P. 1999, MNRAS, 303, 139

Eggleton, P. P. 1983, ApJ, 268, 368

Falcke, H., & Biermann, P. L. 1999, A&A, 342, 49

Fender, R. 2006, In: Compact stellar X-ray sources. Edited by Walter Lewin & Michiel van der Klis. Cambridge Astrophysics Series, No. 39. Cambridge, UK: Cambridge University Press, 381

Homan, J., Buxton, M., Markoff, S., Bailyn, C. D., Nespoli, E., & Belloni, T. 2005, ApJ, 624, 295

Homan, J., & Belloni, T. 2005, Ap&SS, 300, 107

Hynes, R. I., Haswell, C. A., Chaty, S., Shrader, C. R., & Cui, W. 2002, MNRAS, 331, 169

Ichimaru, S. 1977, ApJ, 214, 840

Jahoda, K., Swank, J. H., Giles, A. B., Stark, M. J., Strohmayer, T., Zhang, W., & Morgan, E. H. 1996, Proc. SPIE, 2808, 59

Lasota, J.-P. 2001, New Astronomy Review, 45, 449

Levine, A. M., Bradt, H., Cui, W., Jernigan, J. G., Morgan, E. H., Remillard, R., Shirey, R. E., & Smith, D. A. 1996, ApJ, 469, L33

McClintock, J. E., Horne, K., & Remillard, R. A. 1995, ApJ, 442, 358

McClintock, J. E., & Remillard, R. A. 2006, In: Compact stellar X-ray sources. Edited by Walter Lewin & Michiel van der Klis. Cambridge Astrophysics Series, No. 39. Cambridge, UK: Cambridge University Press, 157

Maccarone, T. J., & Coppi, P. S. 2003, MNRAS, 338, 189

Maccarone, T. J., & Coppi, P. S. 2003, A&A, 399, 1151

Maitra, D., & Bailyn, C. D. 2004, ApJ, 608, 444

Markoff, S., Falcke, H., & Fender, R. 2001, A&A, 372, L25

Markoff, S., Nowak, M. A., & Wilms, J. 2005, ApJ, 635, 1203

Meier, D. L. 2001, ApJ, 548, L9

Migliari, S., & Fender, R. P. 2006, MNRAS, 366, 79

Migliari, S., Tomsick, J. A., Maccarone, T. J., Gallo, E., Fender, R. P., Nelemans, G., & Russell, D. M. 2006, ApJ, 643, L41

Molkov, S. V., Lutovinov, A. A., Cherepashchuk, A. M., & Sunyaev, R. A. 2004, The Astronomer's Telegram, 259, 1

Narayan, R. 2005, Ap&SS, 300, 177

Narayan, R., & Yi, I. 1994, ApJ, 428, L13

O'Brien, K., Horne, K., Hynes, R. I., Chen, W., Haswell, C. A., & Still, M. D. 2002, MNRAS, 334, 426

Predehl, P., & Schmitt, J. H. M. M. 1995, A&A, 293, 889

Rees, M. J., Begelman, M. C., Blandford, R. D., & Phinney, E. S. 1982, Nature, 295, 17

Reig, P., van Straaten, S., & van der Klis, M. 2004, ApJ, 602, 918

Robinson, E. L., Welsh, W. F., & Young, P. 2001, AIP Conf. Proc. 599: X-ray Astronomy: Stellar Endpoints, AGN, and the Diffuse X-ray Background, 599, 902

Rodriguez, J., Shaw, S. E., & Corbel, S. 2006, A&A, 451, 1045

Rupen, M. P., Mioduszewski, A. J., & Dhawan, V. 2004, The Astronomer's Telegram, 286, 1

Russell, D. M., Fender, R. P., Hynes, R. I., Brocksopp, C., Homan, J., Jonker, P. G., & Buxton, M. M. 2006, MNRAS, 371, 1334

Russell, D. M., Fender, R. P., & Jonker, P. G. 2007, MNRAS, 379, 1108

Rutledge, R. E., Bildsten, L., Brown, E. F., Pavlov, G. G., & Zavlin, V. E. 2001, ApJ, 559, 1054

Shakura, N. I., & Sunyaev, R. A. 1973, A&A, 24, 337

Šimon, V. 2002, A&A, 381, 151

Smith, D. A., et al. 2002, ApJS, 141, 415

Sturner, S. J., & Shrader, C. R. 2005, ApJ, 625, 923

van Paradijs, J., & McClintock, J. E. 1994, A&A, 290, 133

Vrtilek, S. D., Raymond, J. C., Garcia, M. R., Verbunt, F., Hasinger, G., & Kurster, M. 1990, A&A, 235, 162

Wachter, S., Hoard, D. W., Bailyn, C. D., Corbel, S., & Kaaret, P. 2002, ApJ, 568, 901

Welsh, W. F., Robinson, E. L., & Young, P. 2000, AJ, 120, 943

van der Klis, M. 2006, In: Compact stellar X-ray sources. Edited by Walter Lewin & Michiel van der Klis. Cambridge Astrophysics Series, No. 39. Cambridge, UK: Cambridge University Press, 39

Yu, W., & Dolence, J. 2007, ApJ, 667, 1043

This preprint was prepared with the AAS LaTeX macros v5.2.

Table 1. Date of peak flux during the outbursts of Aquila X-1 between MJD 50984 – MJD 54411 (1998 June 20 – 2007 Nov 7).

R-band peak (MJD)	J-band peak (MJD)	ASM peak (MJD)	Outburst type: Evolution of light curve morphology	Major Outburst Number
51076	–	–	Mini	–
51320	–	51321	Major: FRED → LIS	1
51676	–	–	Mini	–
51730	–	–	Mini	–
51831	51831	51837	Major: FRED	2
52086	52088	52087	Major: FRED → LIS	3
52192	52192	–	Mini	–
52226	52226	–	Mini	–
52338	–	52336	Major: FRED	4
52707	52711	52705	Major: FRED	5
52923	52923	–	Mini	–
53150	53150	53167	Major: LIS → FRED	6
53268	53268	–	Mini	–
53473	53473	53476	Major: FRED → LIS	7
53579	53580	–	Mini	–
53950	53951	53952	Major: FRED → LIS	8
54242	54245	54253	Major: FRED → LIS	9
54363	54367	54365	Major: FRED → LIS	10

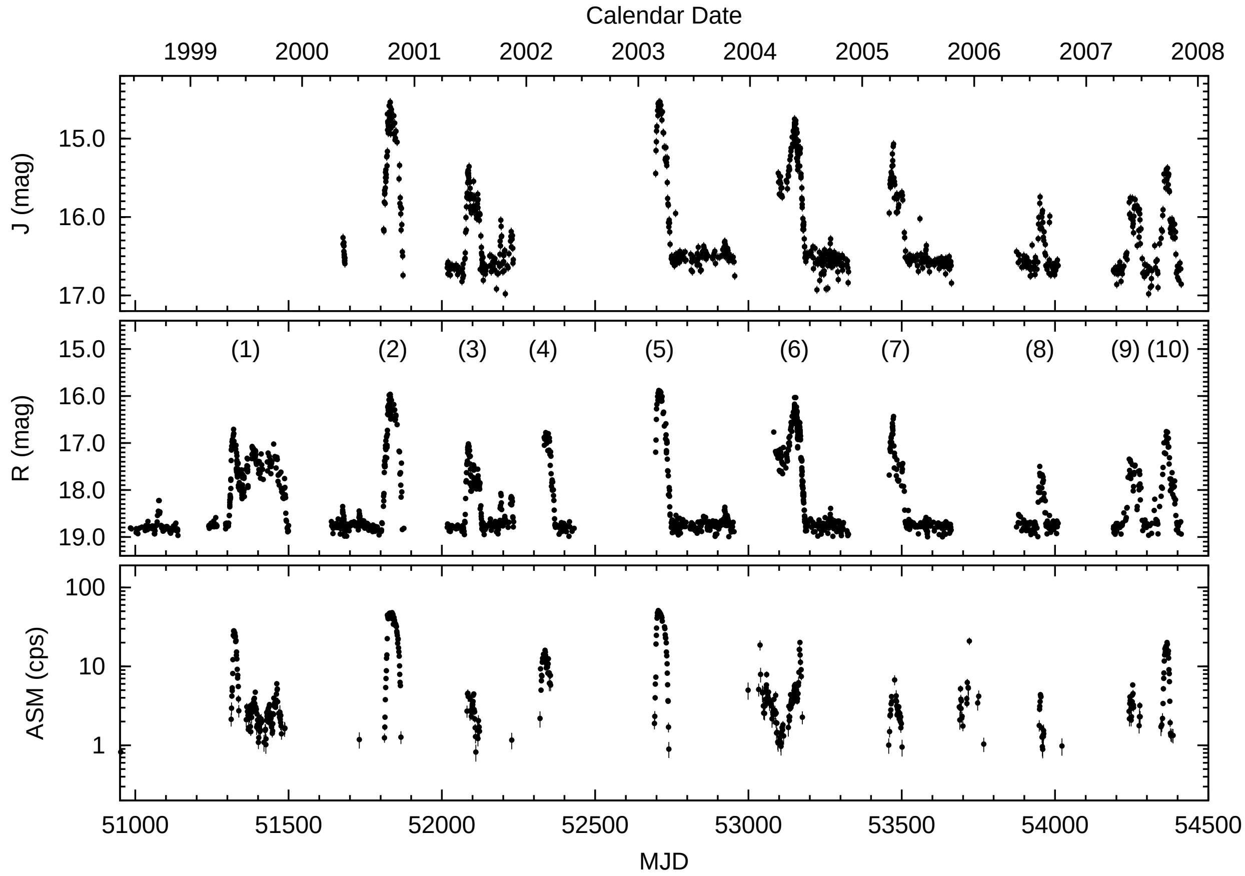

Fig. 1.— Multi-wavelength long-term monitoring of Aquila X-1 between MJD 50984 – MJD 54411 (1998 June 20 – 2007 Nov 7). Top panel: Near-IR J-band light curve. Middle panel: Optical R-band light curve. The numbers in parentheses refer to the serial number assigned to the major outbursts in Table 1. Bottom panel: Logarithm of soft X-ray (∼1.5-12 keV) count-rate as measured by the All-Sky Monitor onboard the RXTE. Since the ASM does not detect the source when in quiescence, only those ASM data are plotted for which the signal-to-noise ratio is > 4. The R and J-band fluxes include the flux from Aquila X-1 as well as from the contaminating star. During periods of quiescence, the soft X-ray flux is below the detection limit of ASM but the combined flux from Aquila X-1+contaminating star remains detectable in both R and J bands. Note that a major outburst which occurred during late 2005 – early 2006 could be seen only with the ASM but not the ground based telescopes due to close angular proximity to the Sun. Therefore we have not labelled this outburst in the middle panel.

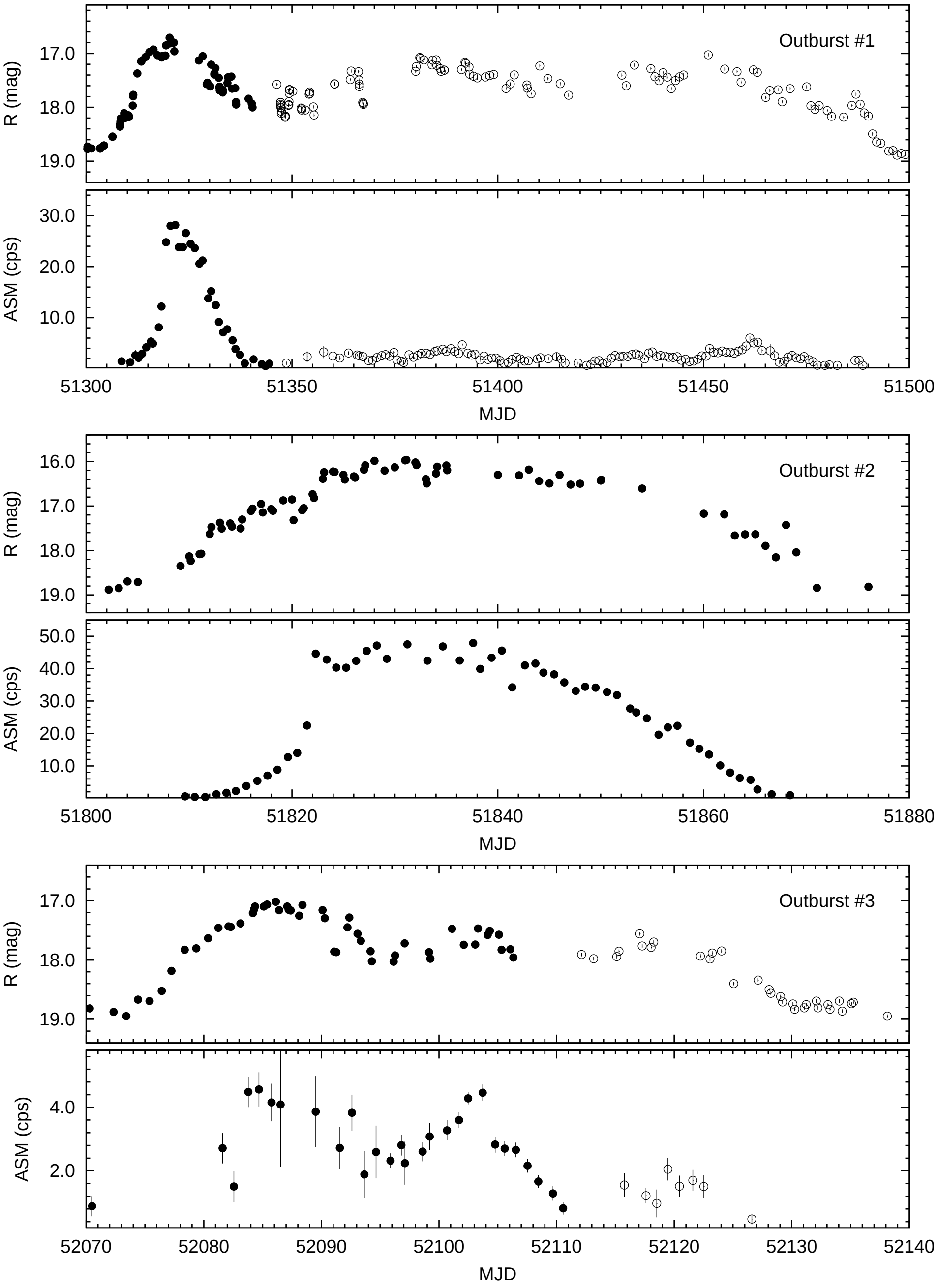

Fig. 2.— Zooming into the R-band and ASM light curves shown in Fig. 1, showing the detailed light curve morphology during major outbursts 1–3. FRED outbursts are marked by filled circles, LIS by open circles. In this figure we are using a linear scale for the ASM count-rates to emphasize the difference between LIS and FRED.

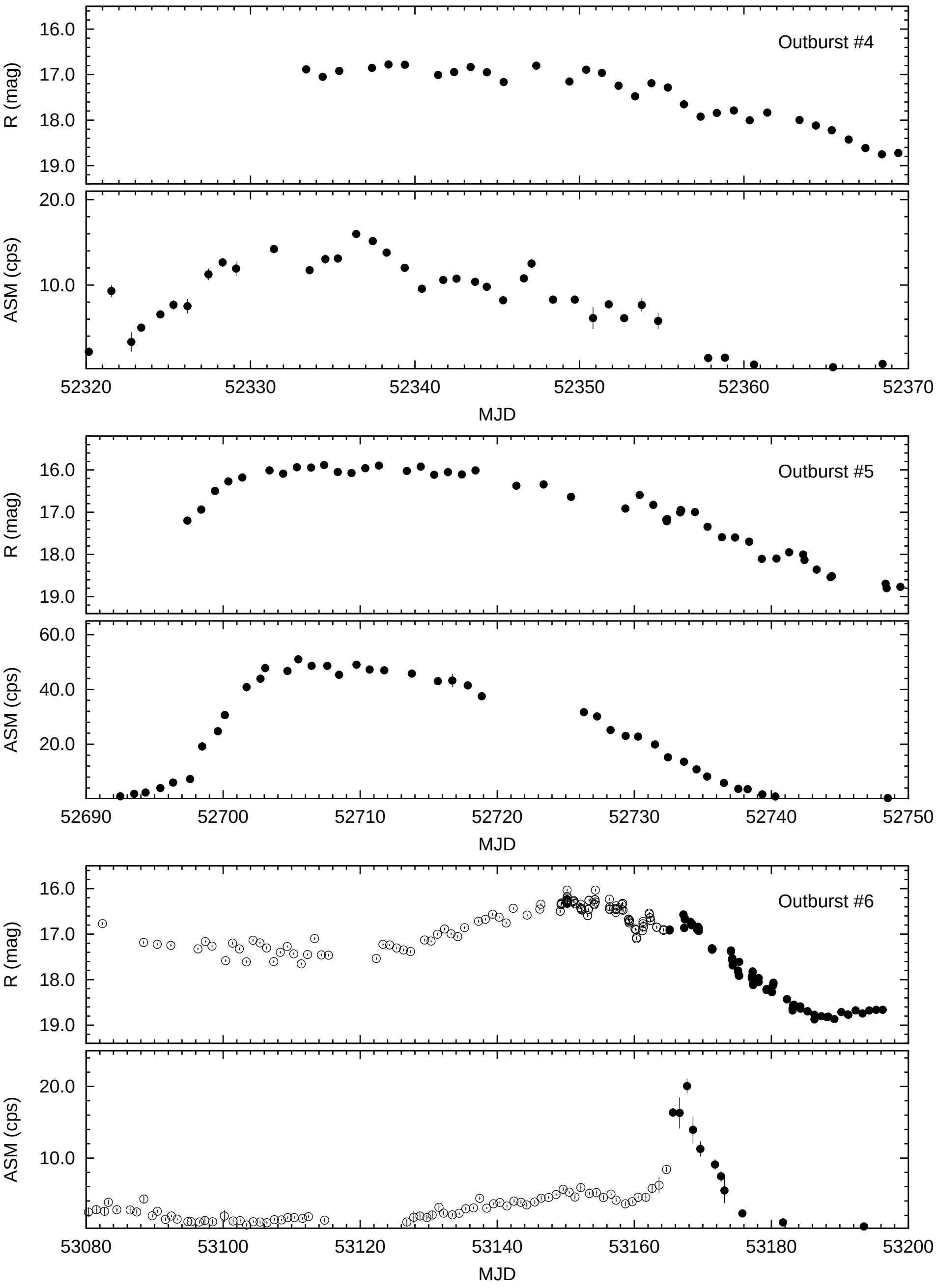

Fig. 3.— Same as Fig. 2, but for outbursts 4–6.

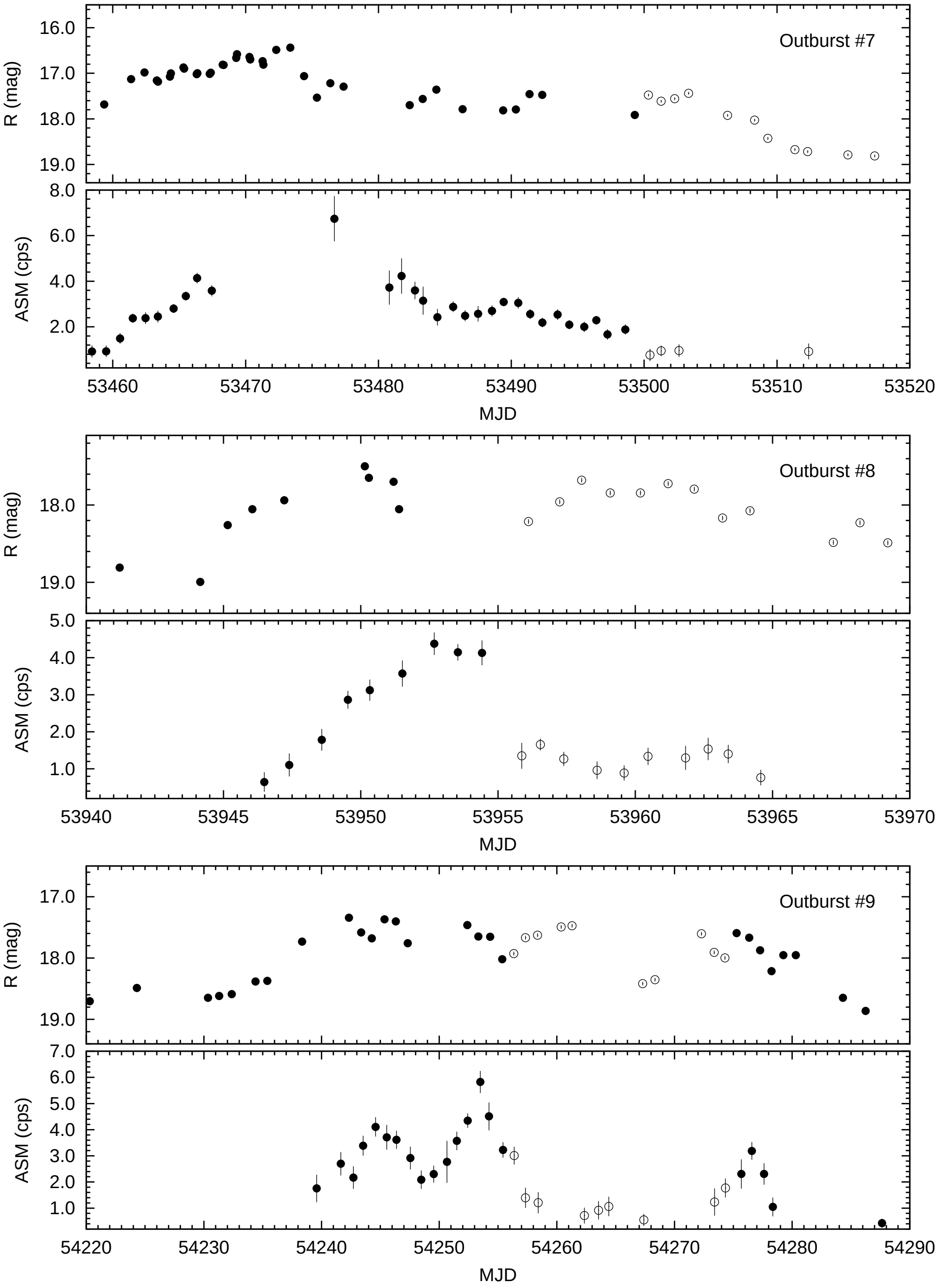

Fig. 4.— Same as Fig. 2, but for outbursts 7–9.

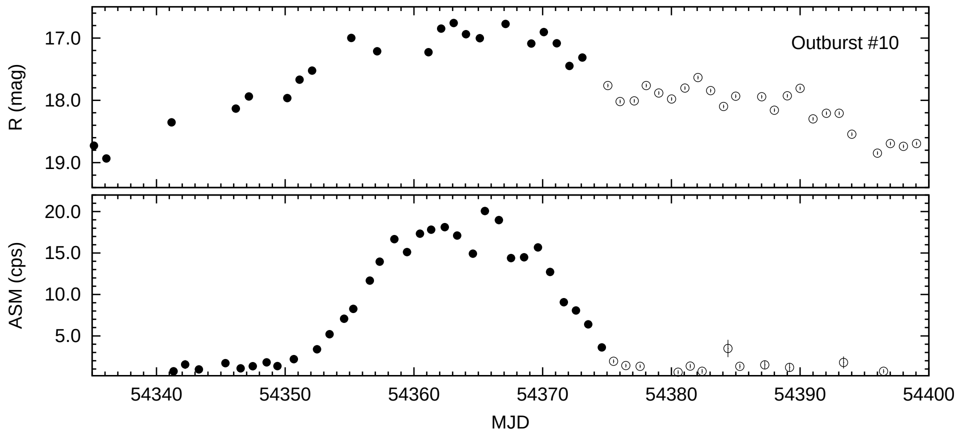

Fig. 5.— Same as Fig. 2, but for outburst 10.

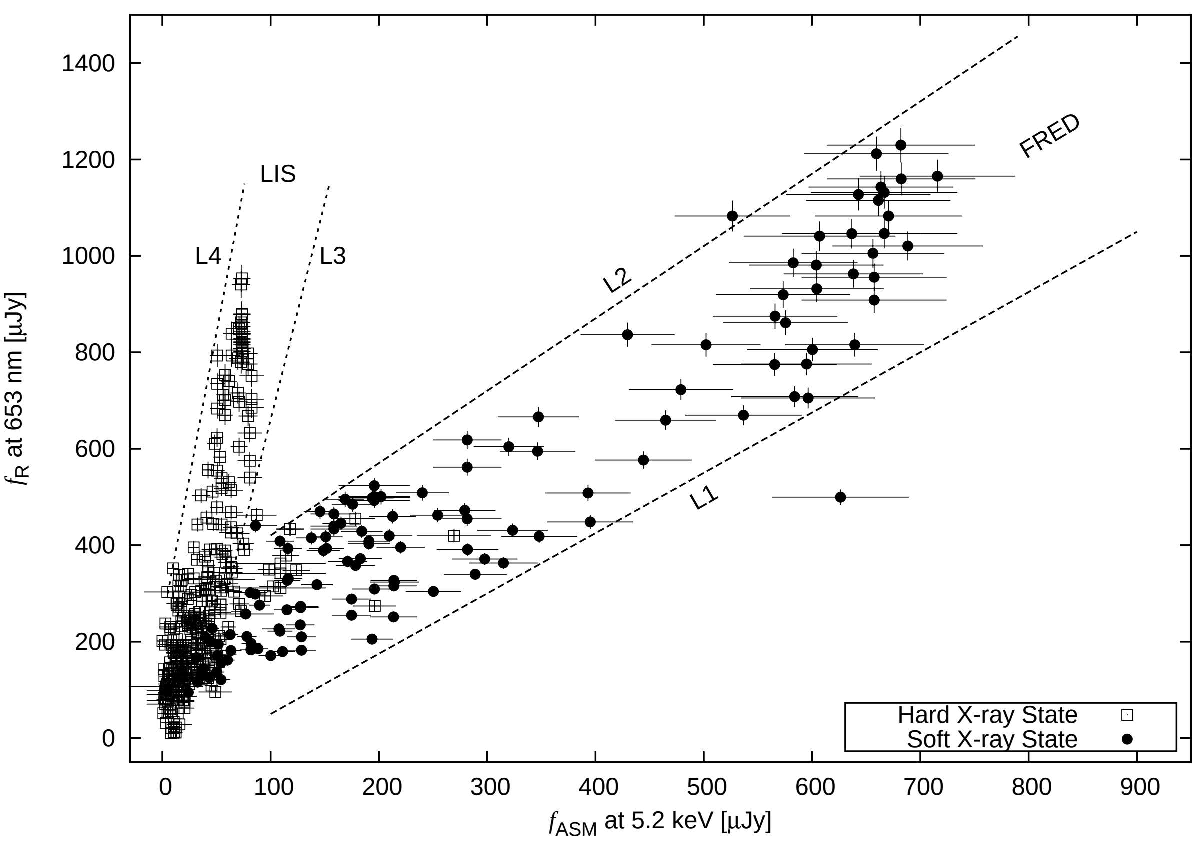

Fig. 6.— Optical–soft-X-ray correlation in Aquila X-1. Data from all the major outbursts from MJD 50984 – MJD 54411 (1998 June 20 – 2007 Nov 7) for which the X-ray state could be determined from contemporaneous RXTE observations (Maccarone & Coppi 2003a,b; Reig et al. 2004; Maitra & Bailyn 2004; Rodriguez et al. 2006; Yu & Dolence 2007, also Manuel Linares, priv. comm.). The dashed lines L1 and L2 which follow the equations $f_R = 1.25 f_{ASM} - 75$ and $f_R = 1.5 f_{ASM} + 270$ respectively, roughly form an envelope containing most of the FRED points. The dotted lines L3 and L4 which follow the equations $f_R = 9 f_{ASM} - 240$ and $f_R = 12 f_{ASM} + 240$ respectively, roughly form an envelope containing most of the LIS points. Filled circles represent data taken during *soft* X-ray state and open squares are those during *hard* X-ray state.

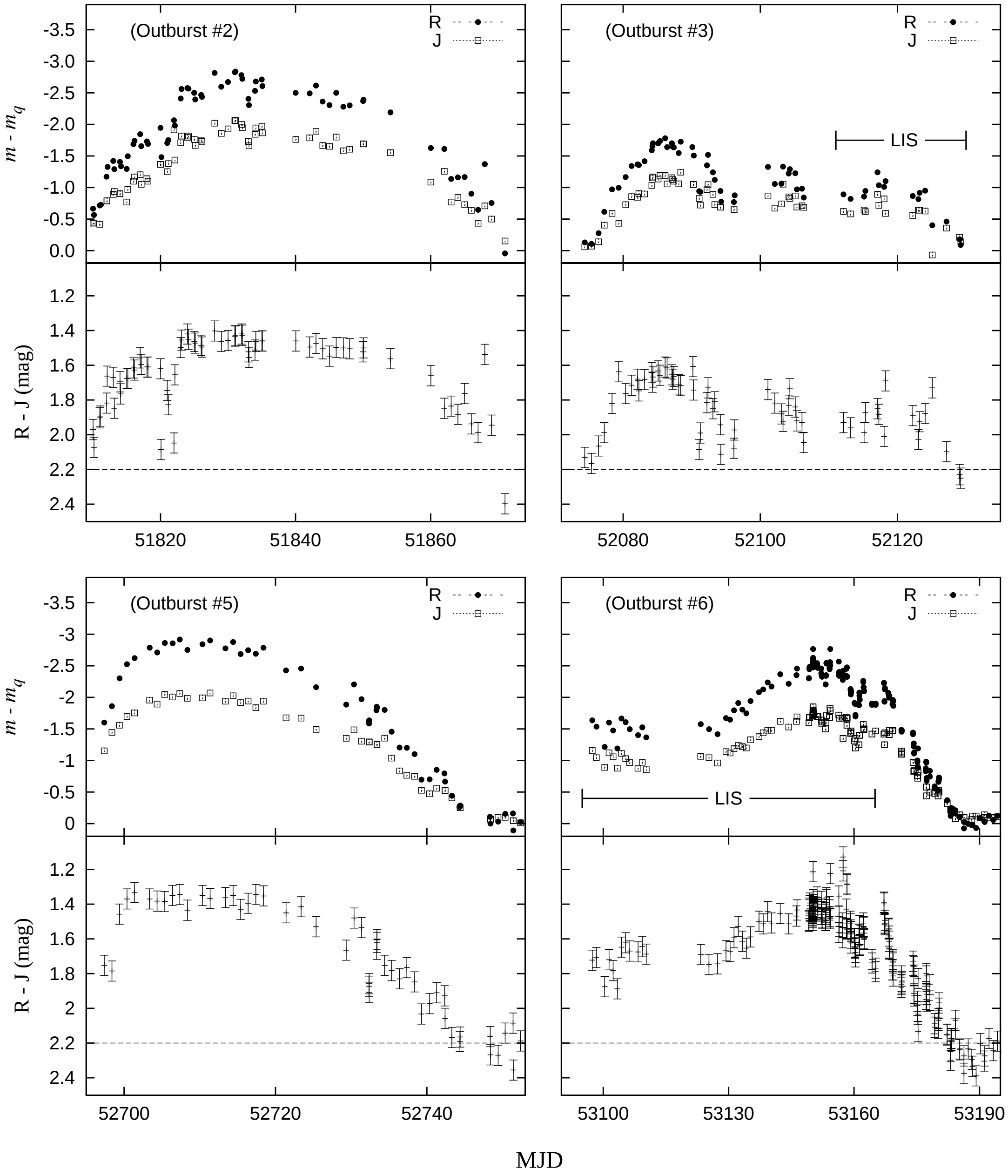

Fig. 7.— Evolution of J-R color during outbursts 2, 3, 5 and 6 of Aquila X-1. The increase in brightness from quiescence is shown in the top panels, with the R-band data shown by filled circles and J-band data shown by open squares. The outburst serial number (Table. 1) is given in parentheses. Variation of corresponding J-R color is shown in the bottom panels. Epochs of LIS as inferred from Figs. 1–5 are labelled. Unless labelled as a LIS, the OIR/soft-X-ray light curve morphology resembles that of FRED outbursts.

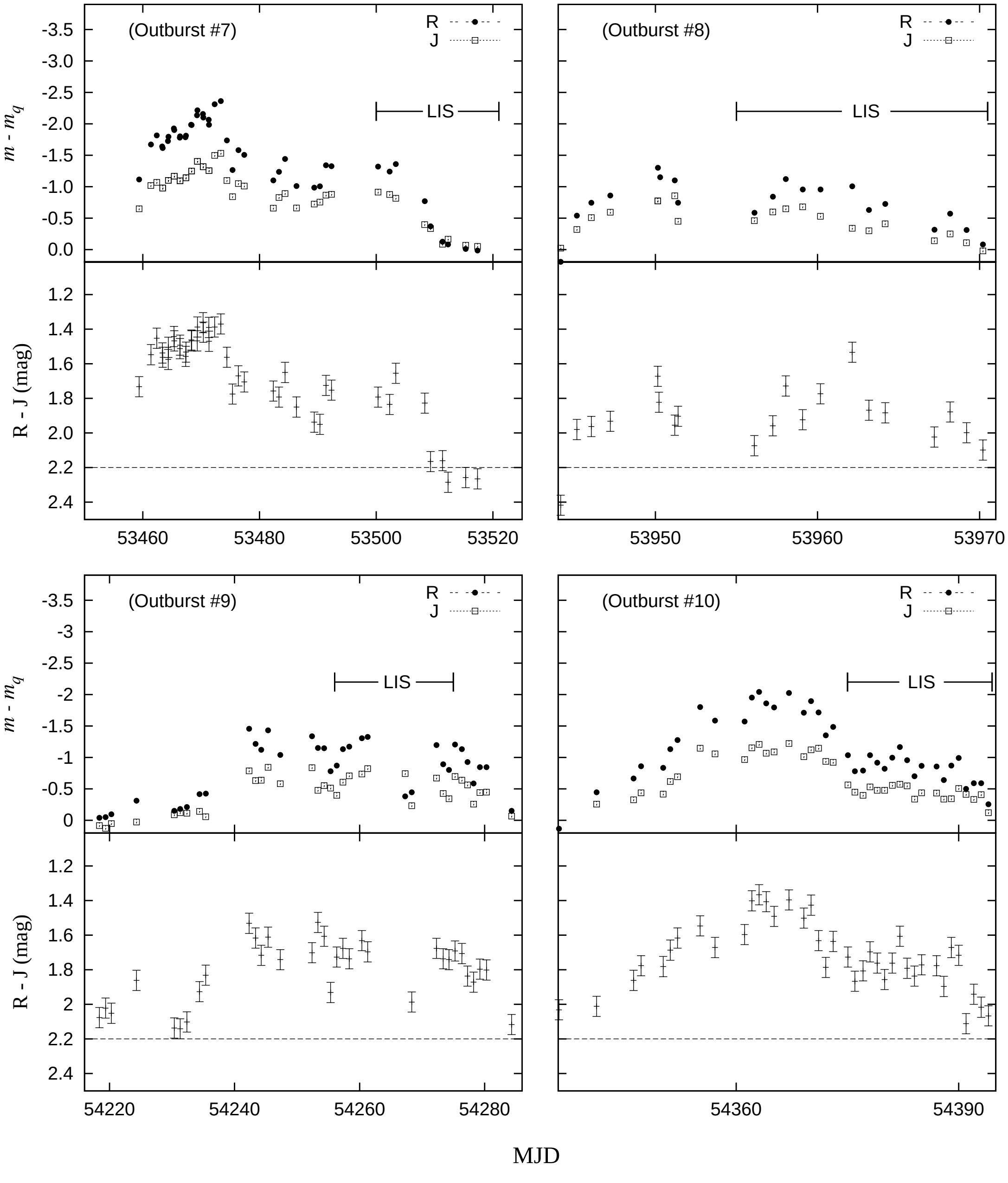

Fig. 8.— Same as Fig. 7, but for outbursts 7–10.

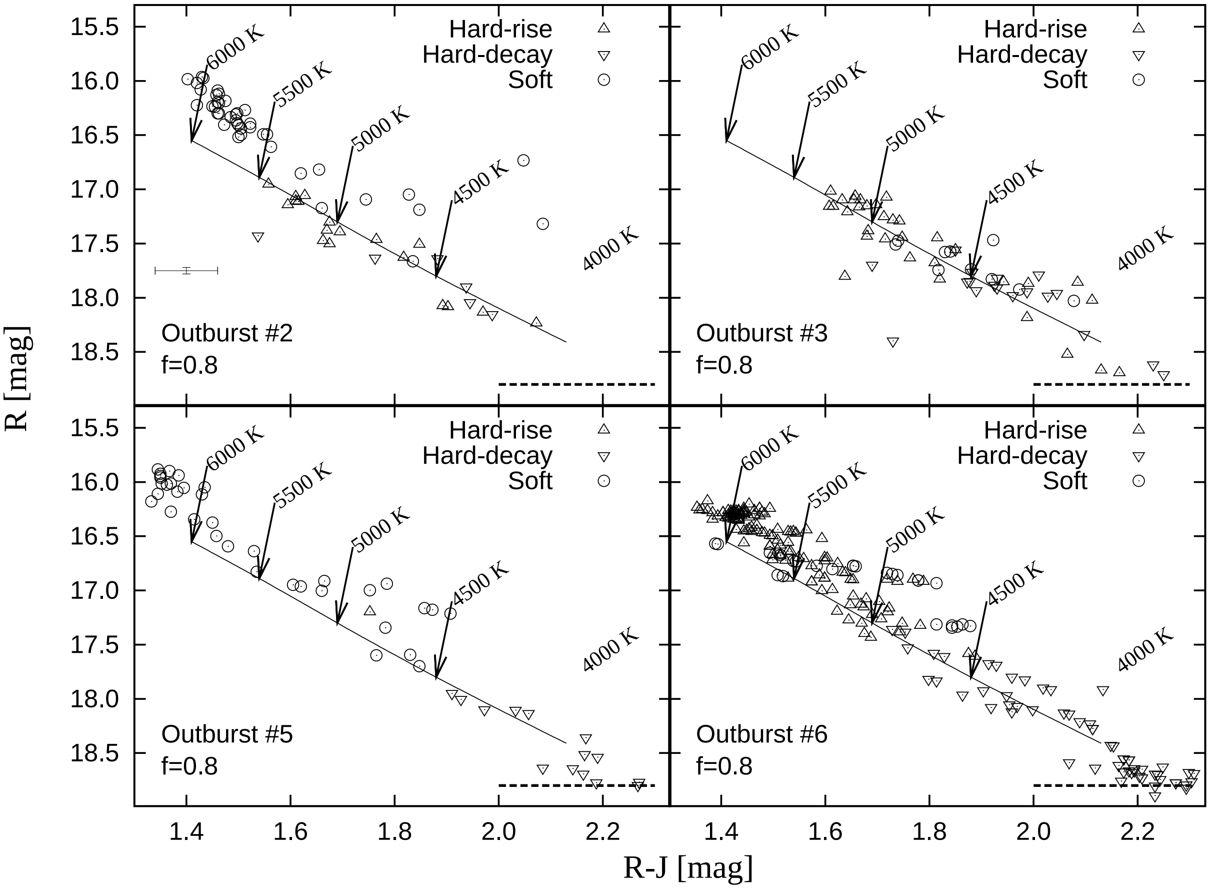

Fig. 9.— Evolution of outbursts 2, 3, 5 and 6 of Aquila X-1 on the OIR color-magnitude diagram. Observations when the source was in hard/power law state during the rise of an outburst are shown by (△). The decaying hard state, are shown by (▽). Outbursts where state transitions were not reported are shown by (□). Observations during soft/thermal dominated state are shown by (○). The quiescent level is shown by the dashed line. A typical error bar is shown in the top left panel near (1.4, 17.75). The solid, curve from bottom-right to top-left in each panel shows the color and brightness expected by heating a disk-shaped blackbody of radius 5 light seconds, inclined to the observer at 45° and at a distance of 3 kpc. The quantity f represents a multiplicative area correction factor. The expected color and magnitude of the disk between temperatures of 4000 –6000 K are labelled.

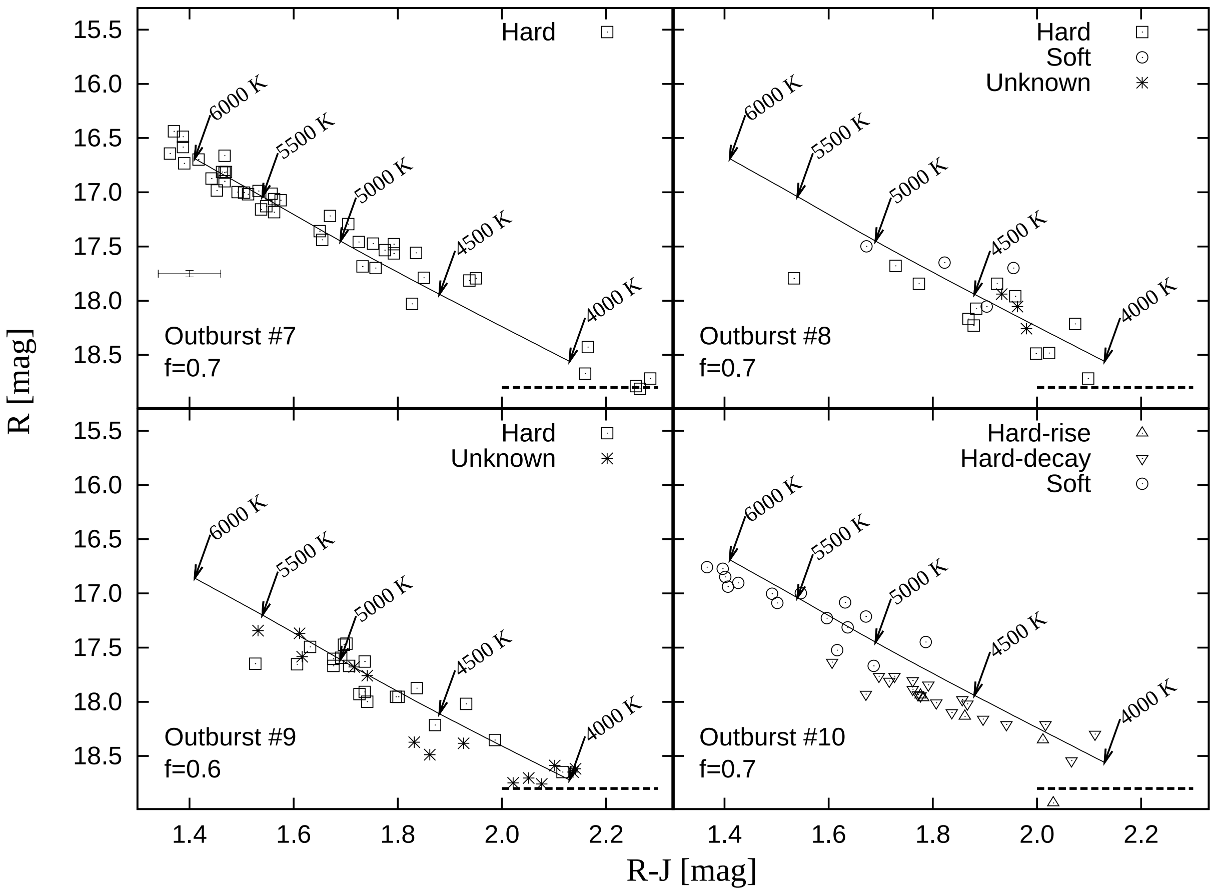

Fig. 10.— Same as Fig. 9, but for outbursts 7, 8, 9 and 10.